Effectiveness assessment of signal processing in the presence of smear

Piet Bijl[1], Jaap A. Beintema[1], J. Dijk[2] & Natasja van der Leden[1]
[1] TNO Defense, Security & Safety: Human Factors, P.O. Box 23, Soesterberg, The Netherlands
[2] TNO Defense, Security & Safety: Observation Systems, P.O. Box 96864, The Hague, The Netherlands
Phone: +31 346 356 277, fax: +31 346 353 977
E-mail: piet.bijl@tno.nl

ABSTRACT

Moving imagery from a static scene was recorded with an un-cooled thermal imager at nine different angular velocities ranging from 0 (static) to 1 pixel/frame (3.75 deg/s) using a tilted rotating mirror. The scene contained a thermal acuity test chart with triangular test patterns based on the Triangle Orientation Discrimination (TOD) test method. The imagery was processed with different types of image enhancement: DSR (Dynamic Super Resolution), LACE (Local Adaptive Contrast Enhancement) and combinations. DSR shows a significant performance improvement at low velocities, a moderate improvement at medium velocities where smear becomes apparent and no benefit at high speed. Performance with LACE is close to optimized gain and level setting by hand. Static performance and dynamic performance at 0.57 pixel/frame containing significant smear were compared with earlier published identification performance data for two-hand held systems collected under a variety of signal processing conditions. It shows that the ratio M_{75} between the 75% correct threshold size for the two-hand held objects and the TOD triangle is preserved under all conditions measured. Thus, TA range prediction based on the TOD is robust against a complex combination of conditions, including motion, smear and the types of image enhancement applied.

Keywords: sensor, thermal imager, signal processing, DSR, LACE, motion, smear, TOD, Acuity, Target Acquisition

1. INTRODUCTION

In a previous study[1], the effect of recording and presentation velocity on the acuity with an un-cooled thermal imager was assessed. The study showed that a slow angular velocity of a TOD[2] test pattern over the sensor focal plane (up to 0.25 pixel/frame) results in a large acuity increase (+ 50%) compared to the static condition. This can be understood because the observer is able to utilize more phases of the same test pattern. At higher sensor velocities the benefit rapidly decreases due to sensor smear and above 0.50 pixel/frame the difference with the static condition is marginal. Up to 0.75 pixel/frame, performance was hardly affected by the playback speed indicating that temporal display characteristics and human dynamic acuity are not responsible for the reduction.

The results are in agreement with the general finding[3-8] that motion with under-sampled cameras can significantly increase observer performance and at the same time provide a quantitative explanation for the marginal performance difference between the identification of hand held objects in static and dynamic imagery reported by Beintema et al.[9]. As explained, the latter is the only study performed with an un-cooled thermal imager moving at a speed of 0.57 pixel/frame and hence the results are considerably affected by detector smear.

In the present study the experiments performed by Bijl[1] are repeated but now with several types of DSR (Dynamic Super Resolution), LACE (Local Adaptive Contrast Enhancement) and combinations applied to the image set. The purpose is twofold. First, we want to characterize how well signal processing techniques perform under all these conditions and deal with smear. Second, with the static scene and with a speed of 0.57 pixel/frame we can directly compare TOD acuity with the identification results for two-hand held objects under all these conditions obtained by Beintema et al.[9]. This yields the TOD magnification factor M_{75} for identification of two-hand held objects and shows how well this factor is preserved under complex combinations of signal processing and smear.

Infrared Imaging Systems: Design, Analysis, Modeling, and Testing XXI, edited by Gerald C. Holst, Keith A. Krapels,
Proc. of SPIE Vol. 7662, 76620E · © 2010 SPIE · CCC code: 0277-786X/10/$18 · doi: 10.1117/12.850132

The paper is organized as follows. Methods are described in Chapter 2. The results are provided in Chapter 3. In Chapter 4, a direct comparison between TOD acuity and identification performance for real objects is made. The results are discussed in Chapter 5.

2. METHODS

The setup is similar to the one used by Bijl et al.[5] and Beintema et al.[9] except for some minor differences that will be indicated in the text below.

2.1 IMAGE COLLECTION

A FLIR SC2000 under-sampled, un-cooled microbolometer sensor with a focal plane array of 320 by 240 pixels (see Figure 1a) was used. Camera Field Of View (FOV) is 24 by 18 degrees. The camera gives a calibrated output of the temperatures in the scene and is regularly calibrated according to the TNO laboratory quality program. Digital output data (14-bit) is recorded on a computer at a frame rate of 50 Hz. The detector time constant is 12 ms.

A surface mirror was placed in front of the camera objective under an angle of approximately 45 degrees (see Figure 1a) so that an image was obtained with the test pattern in the center (see below). The mirror was mounted on the axis of an electric motor and slightly tilted with respect to the rotation axis in order to produce a circular motion of the image. Diameter and speed are set by the changing the tilt angle and rotation frequency. A circular motion is convenient and has several advantages over a translation: the magnitude of the velocity is constant and the target remains within a limited area of the sensor FOV.

Thermal test patterns were generated with the TCAT or Thermal Camera Acuity Tester[10] (see Figure 1b). The test plate consists of five lines with four thermal triangle test patterns of arbitrary orientation on each line. The test patterns at the top line are the largest (triangle base = 20 mm, or triangle square-root area S = 13.2 mm) and every next line the test pattern size decreases by a factor of 1.19, so that the test pattern size decreases by a factor of two over the plate. The test plate was placed in the apparatus in four different orientations, which enhances the number of possible test pattern presentations and makes learning by heart more difficult. The TCAT was placed at two ranges (D_1 = 4.86 m and D_2 = 8.17 m) from the sensor, resulting in eight different angular test pattern sizes (the smallest two sizes at D_1 coincide with the two largest sizes at D_2). At D_1, test pattern size S ranges from 2.72-1.36 mrad (S^{-1} = 0.37 -0.74 mrad^{-1}), and at D_2, test pattern size S ranges from 1.62-0.81mrad (S^{-1} = 0.62 -1.24 mrad^{-1}). Thermal contrast was ΔT =1.93 K. This value was determined using the thermal imager. In this contrast region camera acuity is largely insensitive to thermal contrast because it is high compared to the camera noise[5]. Note that the measured contrast includes possible losses due to the surface mirror.

(a) (b)

Figure 1. a: Camera and the rotating tilted mirror used to generate a dynamic image. b: the TCAT used to generate the thermal test patterns.

Both static (50 frames) and dynamic recordings (250 frames) were made. For the dynamic recordings, the radius of the circular motion was approximately 4 pixels or 5.2 mrad (this is slightly different from the experiments by Bijl et al.[5] and Beintema et al.[9]), and rotation frequency was varied in such a way that the velocity of the TCAT over the sensor Focal Plane Array was 0, 0.125, 0.25, 0.375, 0.50, 0.625, 0.75, 0.875 and 1.0 pixel/frame. Example recordings are shown in Figure 2. The left-hand side picture shows a static recording of the TCAT test apparatus while the right-hand side picture shows the same scene but now recorded at a speed of 0.75 pixel/frame. The latter image clearly shows a smear behind the triangle test patterns and even the top triangles are hard to judge.

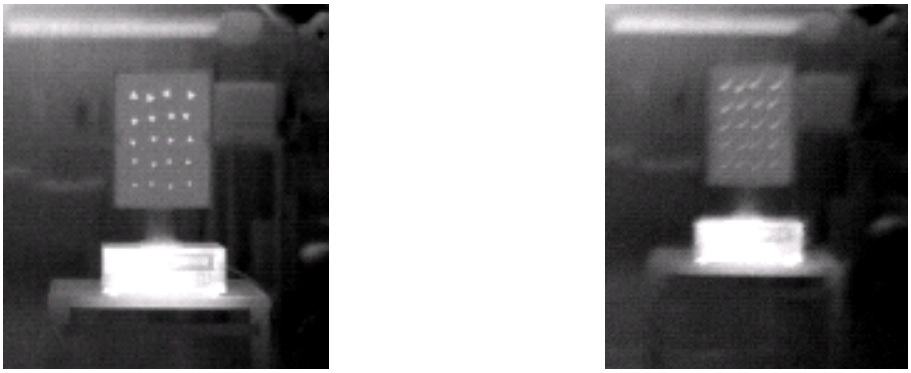

(a) (b)

Figure 2. Examples of the triangle test pattern images. a: static image. b: same scene, but now recorded at a speed of 0.75 pixel per frame. The right image clearly shows a smear behind the triangle test patterns and even the top triangles are hard to judge.

2.2 SIGNAL PROCESSING

Seven different conditions are used in this study. These conditions and the relative image sizes on the screen are listed in Table 1. The 'Normal' condition is unprocessed. The 'Enlarged' condition is equal to the normal one but with the image size magnified two times using bilinear interpolation as in the study by Bijl[1]. This condition is added to be able to disentangle the effect of super-resolution from the pure scaling effect of DSR2[5] (see below) and should be comparable to the condition in Bijl[1]. Two types of super-resolution are applied: DSR2[13] effectively results in a reduction of the detector pitch by a factor of 2 and a doubling of the pixel resolution. DSR4[13] reduces the pitch by ¼ and results in a fourfold pixel resolution. In addition, the normal and two DSR conditions are also processed with the LACE[13] algorithm.

Table 1: Normal and signal processing conditions used in this study. See text for details.

Conditions	Additional magnification factor	Total magnification
Normal	1	1
Normal + LACE	1	1
Enlarged	2	2
DSR2	1	2
DSR2 + LACE	1	2
DSR4	1	4
DSR4 + LACE	1	4

2.3 PERCEPTION TEST

The observer experiments were carried out in a dimly lit room. As in the study of Beintema et al.[9], test patterns were shown on a 22-inch computer CRT set at a resolution of 1024 by 768 pixels. The display differs in size and resolution from the one used in the study by Bijl[1]. In order to obtain a good test pattern contrast on the display for the Normal, Enlarged, DSR2 and DSR4 sequences, the 8-bit grey values shown on the display were assigned to a linear temperature range between 19.0°C (approximately 25% below the TCAT background temperature) to 23.1°C (25% above the test pattern temperature). For the conditions processed with LACE, no manual optimization was performed. In addition, display contrast and brightness were optimized in advance by the experimenter such that a zero grey level was just visible and a maximum grey level was just not saturated. The observers were not allowed to touch the display controls. They were free to choose the optimum distance from the display (most of the time distance was approximately 50 cm). In order to equally divide learning effects over the different conditions, the image sequences were divided over four blocks. Each block contained the same set of sequences except that the test plate orientations of the TCAT were different (these were also randomly divided over the blocks).The blocks were presented in different order to the observers according to a 4 by 4 Latin Square design[11] and finally the order inside the blocks was shuffled. For each image sequence, the observers had to indicate the orientation of all 20 triangles on the test chart.

Five observers between 20 and 33 years old participated in the experiment: MS, MR, WJ, AS and NL. All observers had normal or corrected to normal vision.

For each signal processing condition (7), velocity (9) and observer (5), 160 responses were collected (5 test pattern sizes with 16 targets per size at two ranges). Thus, the total amount of responses is 50400. The experiment took about 5 hours per observer, subdivided into 6 sessions of 40-60 minutes.

2.4 DATA ANALYSIS

A Weibull function was fitted through each set of 160 responses using a maximum likelihood procedure, resulting in a 75% correct threshold triangle size (in mrad) and standard error[12]. Finally, a weighted average was calculated across observers. The maximum of the internal error (due to the uncertainty in the individual threshold estimates) and the external error (due to the differences in observers) was used as the error in the resulting thresholds.

3. RESULTS

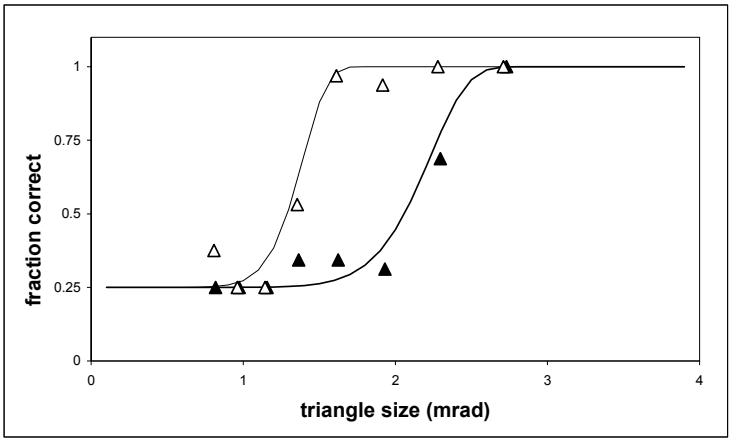

Figure 3. Probability correct versus test pattern size for two conditions: static (filled triangles) and DSR4 with the scene moving over the sensor Focal Plane with 0.125 pixel/frame (open triangles). Observer MS. Maximum likelihood fits are indicated by the continuous curves.

3.1 RAW DATA ANALYSIS

As an example, Figure 3 shows the fraction correct versus triangle test pattern size (in mrad) for two conditions for observer MS. Filled triangles represent the static condition; open triangles represent a dynamic condition with a recording velocity 0.125 pixel/frame and DSR4 super resolution applied. Maximum likelihood fits of the Weibull function are indicated by the continuous curves. The corresponding 75% correct thresholds sizes are S = 2.33 ± 0.08 mrad (S^{-1} = 0.429 ± 0.015) and S = 1.46 ± 0.04 mrad (S^{-1} = 0.685 ± 0.018).

Thresholds from one observer (AS) deviated more than 3 standard deviations from the average over a large number of conditions. For this reason, the data from this observer were excluded from further analysis.

3.2 OVERALL RESULTS

Figure 4 shows the overall results of the study. For each of the 7 conditions, TOD acuity (in mrad^{-1}) is shown as a function of the velocity of the sensor over the test patterns (in pixels/frame). The weighted average over the observers is shown. Error bars indicate the maximum of the internal and external error (see 2.4). In general, the errors are very small: 1-3% except for some data points at the two highest velocities.

All data points at zero speed coincide nicely at a threshold acuity between 0.40-0.44 mrad^{-1}, in agreement with the findings by Bijl[1] but somewhat lower than the result by Bijl et al.[5]. This acuity corresponds to a threshold triangle size S = 1.91-1.74 times the sensor pixel pitch. In the static condition, no improvement of DSR is expected. An increase in display size nor the application of LACE has a strong effect on static acuity.

For all conditions, a slow sensor motion (1/8th – 1/4th pixel/frame) increases performance compared to static imaging. If speed increases further, the improvement decreases due to the occurrence of smear. Without signal processing, the net result of motion is zero at speeds around 0.4-0.6 pixel/frame. These findings are in qualitative agreement with earlier studies[1,5].

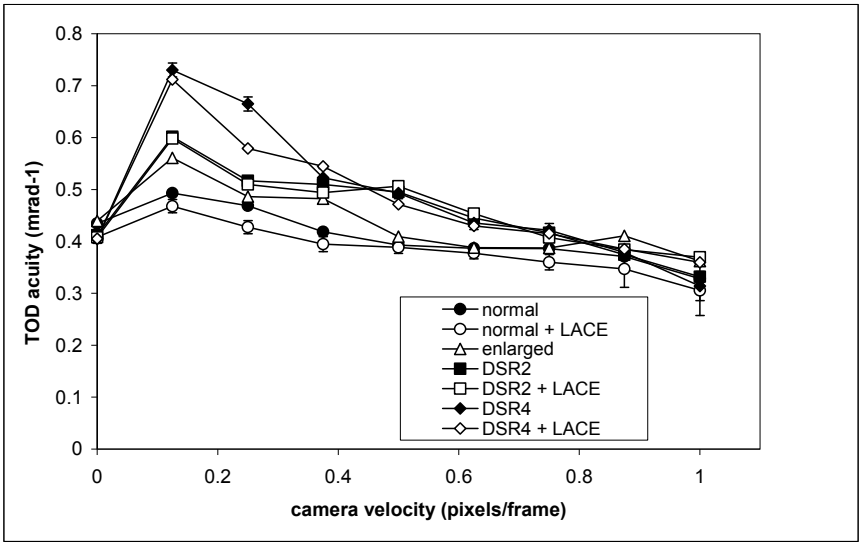

Figure 4. TOD acuity (in mrad^{-1}) as a function of the velocity of the sensor over the test pattern (in pixels/frame). The data from one observer were excluded from the analysis (see text). The weighted average over the other four observers is shown.

The performance increase found with the normal condition (filled circles) is less than reported by Bijl[1]. This can be ascribed to a different image size and different display properties. In the earlier studies[1,5], care was taken that performance was not limited by display properties by doubling the image size and by using a low resolution display setting. In the present study, a more commonly used display setting was used as in Beintema et al.[9]. Under these circumstances, performance is partly limited by the display properties and the maximum benefit from the different phases during motion can not be achieved. As can be seen in Figure 4, the improvement due to motion in the condition with enlarged image (open triangles) is indeed much larger (see also the next section).

3.3 SUPER RESOLUTION

In Figure 5, the relative acuity of the conditions Enlarged (open triangles), DSR2 (filled squares) and DSR4 (filled diamonds) compared to the normal condition are plotted as a function of sensor velocity over the test pattern (in pixels/frame). The data are calculated from the data shown in Figure 4.

Enlarging the image by a factor of two has a positive effect of 0-15% on TOD acuity, although the effect does not seem to depend systematically on velocity. The result is different from the findings in Bijl[1] and Bijl et al.[5]. This is expected: in these studies display and image size were chosen in such a way that enlargement had no effect. At medium (0.4-0.6 pixel/frame) and high (> 0.6 pixel/frame) velocities, enlargement has a limited effect on performance.

The performance increase with DSR2 at low image velocities is around 15-25%. This is partly a result of the increased image size (see above); the remainder (about 10%) can be ascribed to the specific super- resolution algorithm properties. A direct comparison with the study from Bijl et al.[5] cannot be made because of the different display properties but the results of Bijl et al. (+ 18%) fall well between the ratio DSR2/normal and DSR2/enlarged. At medium velocities (0.4-0.6 pixel/frame) DSR2 shows a pronounced increase of 20-30% compared to the normal sequence, while just increasing image size has no effect. Thus, the application of DSR2 is beneficial in this area. At high velocities the effect of DSR2 is marginal.

The application of DSR4 is very beneficial at low image velocities (around 50%) and comparable to DSR2 at medium (20%-30%) and high velocities (no benefit).

In summary, DSR has a strong effect at low velocities (especially the 4 by 4 algorithm), a medium effect at medium velocities where smear occurs, and no effect at high velocities.

3.4 LOCAL ADAPTIVE CONTRAST ENHANCEMENT

In Figure 6, the effect of LACE compared to manually optimized imagery on acuity is shown as a function of the velocity of the sensor over the test patterns (in pixels/frame). Open circles represent a normal image sequence, open squares represent sequences with DSR2 and open diamonds with DSR4. Data are calculated from Figure 4.

For the normal sequences, LACE results in a slightly lower acuity than manual optimization (-5%), independent of velocity. With DSR2 and DSR4, the effect is negligible over the entire velocity range.

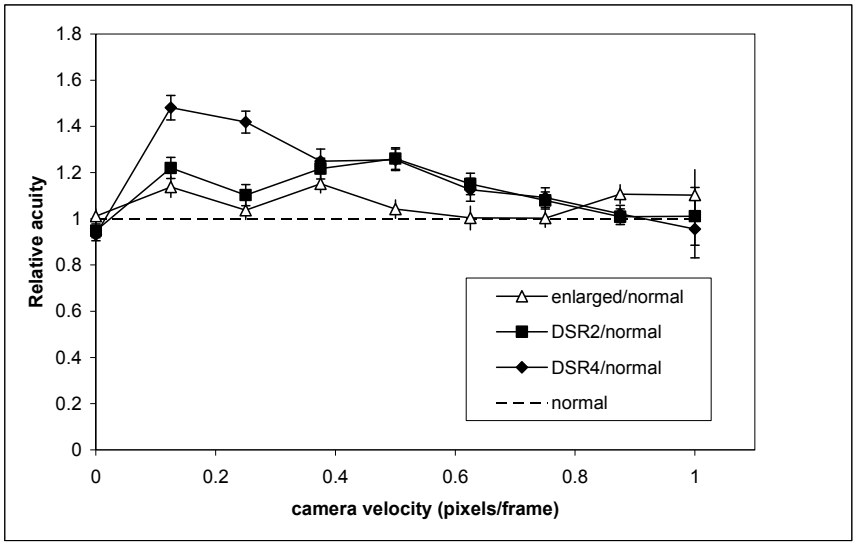

Figure 5: Relative acuity of the conditions Enlarged (open triangles), DSR2 (filled squares) and DSR4 (filled diamonds) compared to the normal condition as a function of the velocity of the sensor over the test patterns (in pixels/frame). Data are calculated from Figure 4.

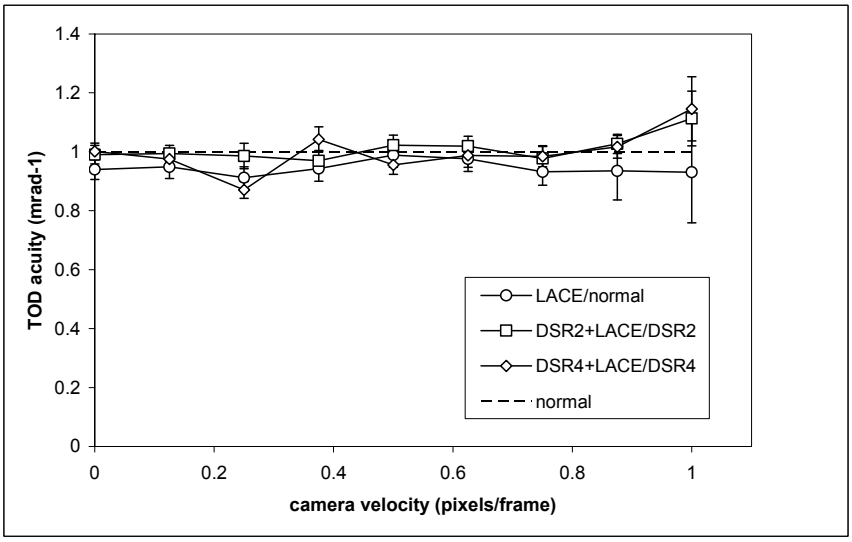

Figure 6: Acuity with LACE compared to manually optimized sequences as a function of the velocity of the sensor over the test patterns (in pixels/frame). Open circles: normal image sequence; Open squares: sequences with DSR2; Open diamonds: sequences with DSR4. Data are calculated from Figure 4.

4. TOD VERSUS REAL TARGET ID

In their study, Beintema et al.[9] present 75% correct identification ranges for a set of two-hand held objects shown at +/- 45 degrees aspect angle for a variety of signal processing techniques. Camera velocities were 0 and 0.57 pixel/frame. Characteristic thermal contrast for their set is approximately 2.0 K which is very close to the contrast of the TOD test patterns used in this study, and target characteristic size is 0.255 m. Note that we used the same display in the two studies.

Two static and five dynamic conditions from their two-hand held target ID study can be compared to the experimental conditions in the present TOD study, except that the velocities do not exactly match. In order to make a comparison at 0.57 pixel/frame, we average the TOD data for 0.50 and 0.625 pixel/frame from the present study.

Next, we calculate the ratio M_{75} between the target characteristic angular size at 75% correct for the hand-held objects and the TOD tests patterns for each of the seven conditions. The experimental error (4-7%) is mainly determined by the error in the ID data (4-6.5%) and slightly by the TOD data (1-3%).

The results are shown in Figure 7. M_{75} is shown for two static and five dynamic conditions containing smear. The conditions include DSR2, DSR4, LACE and combined signal processing. The continuous line indicates the weighted average of M_{75} =4.92 ± 0.16 over all conditions. All estimates deviate less than two times their standard error and less than 10% from the average, showing that M_{75} is essentially independent from the experimental conditions.

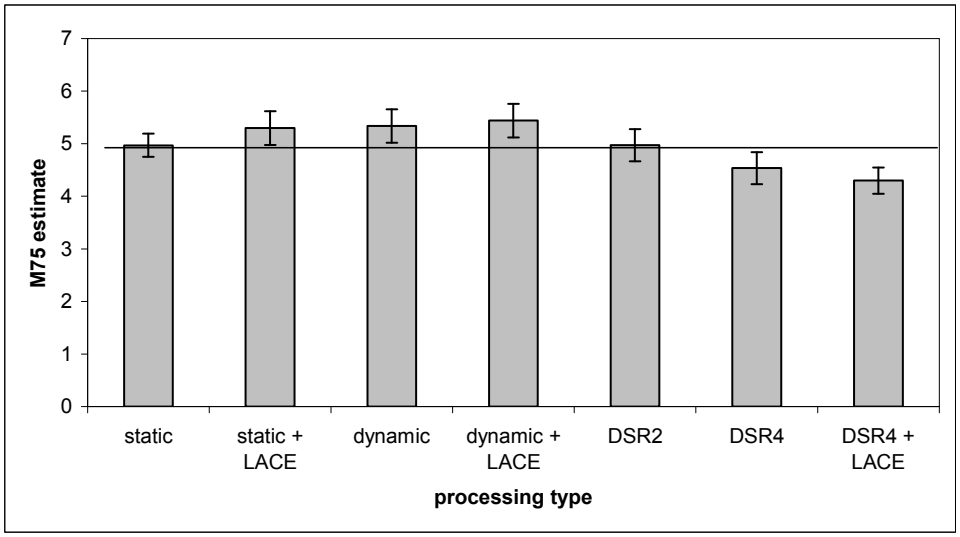

Figure 7. M_{75} or the ratio between the two-hand held ID object size[9] and the TOD threshold size (this study) at the 75% correct level for a variety of static and dynamic conditions. The experimental error in the data is 4-7%. The continuous line indicates the weighted average of M_{75} over all conditions. All estimates deviate less than 2 times the standard deviation and less than 10% from the average, showing that M_{75} is independent from the experimental conditions including motion, signal processing and smear.

5. DISCUSSION AND CONCLUSIONS

In this study we determined the relationship between sensor velocity and TOD acuity for a variety of signal processing techniques applied to an un-cooled thermal imager. The results can be used to estimate the effectiveness of these signal processing techniques under different circumstances.

An important result of the study is that the apparent paradoxal ID results from Beintema et al.[9] for two-hand held objects (no improvement with motion and limited improvement with DSR) are in excellent quantitative agreement with the current results for the TOD acuity and can easily be explained with the presence of smear at the chosen sensor velocity.

With this study the robustness of the relationship between the TOD test and identification of real objects is again shown. In the present study both static and dynamic scenes were presented, including smear, DSR, LACE and combinations. Note that this is a strong result because the sensor system characteristics differ widely from condition to condition: the static imagery are under-sampled, the dynamic imagery without DSR are under-sampled but contain smear, and the DSR imagery are welll-sampled and contain smear.

The ratio between the threshold target characteristic angular size for two-hand held targets at 45 degrees aspect angle and the TOD triangle size $M_{75} = 4.92 \pm 0.16$ over all conditions. Since TA range for two-hand held objects as a function of aspect angle does not exactly match the predictions made by the models that use the target square-root area assumption[2,9,14], a conversion factor is required to obtain the average M_{75} over all aspect angles. From Beintema et al.[9], figure 8, we can deduce that this factor equals 1.43 for the five aspect angles used in their experiment. As a result, M_{75} =7.0 over these aspect angles. Conversion[15] to the TTP metric yields $V_{50} = 7.0/0.58 = 12.1$.This is a little lower than the value estimated from an earlier study with a similar target set[16].

DSR can significantly improve performance for un-cooled thermal imagers at low velocities and moderately at medium velocities. Performance appears to be limited by the occurrence of smear. With the sensor under test (FOV = 24 by 18 degrees), performance reduction already appears at velocities above approximately 1 deg/s. However, with an adapted super resolution algorithm the amount of smear may be calculated and corrected for based on the temporal characteristics of the detectors and the velocity estimate performed in any super resolution algorithm,. This may lead to a more effective algorithm for low-cost (un-cooled) sensors at medium and high velocities. In addition, it may permit faster scanning and therefor significantly improve search perfomance with these type of systems. The performance of such an algorithm may be quantified using the method described in this study. Moreover, application to the collected image set with the TOD test pattern and the two-hand held objects may further validate the TOD robustness.

Application of LACE compared to manual optimization had a minor negative effect (-5%) on the performance for unprocessed images and no effect on the images processed with DSR2 and DSR4. This is a good result since LACE has several advantages to manual optimization: optimization is automatic, and optimum performance can be expected any time and anywhere in the scene.

REFERENCES

1. Bijl, P. (2010). Visual Image Quality Assessment with sensor motion: Effect of Recording and Presentation Velocity. Applied Optics, Vol. 49, Issue 3, pp. 343-349.
2. P.Bijl and J.M. Valeton, “TOD, the alternative to MRTD and MRC,” Optical Engineering 37, 7, 1976 – 1983 (1998).
3. R.G. Driggers, K. Krapels, S. Murrill, S.S. Young, M. Thielke, and J. Schuler, “Superresolution performance for undersampled imagers,” Optical Engineering 44, 1 (2004).
4. K. Krapels, R.G. Driggers and B. Teaney, B., “Target-acquisition performance in under-sampled infrared imagers: static imagery to motion video,” Applied Optics, 44 (33), 7055-7061 (2005).
5. P.Bijl, K.Schutte and M.A. Hogervorst, “Applicability of TOD, MRT, DMRT and MTDP for dynamic image enhancement techniques,” Proc SPIE **6207**, 154-165 (2006).
6. M.A. Hogervorst, A Toet and P. Bijl,. (2006). The TOD method for dynamic image quality assessment. (Report TNO-DV 2006 C423). Soesterberg, The Netherlands: TNO Defence, Security and Safety.

7. J. Fanning, J. Miller, J. Park, G. Tener, J. Reynolds, P. O'Shea, C. Halford, and R. Driggers, "IR system field performance with superresolution," Proc SPIE **6543**, 65430Z (2007)
8. S. Hu, S. S. Young, T. Hong, J.P. Reynolds, K. Krapels, B. Miller, J. Thomas, and O. Nguyen (2010). Super-resolution for flash ladar imagery. Applied Optics, Vol. 49, Issue 5, pp. 772-780
9. Beintema, J.A., Bijl, P., Hogervorst, M.A. & Dijk, J. (2008). Target Acquisition performance: effects of target aspect angle, dynamic imaging and signal processing. In: Infrared Imaging Systems: Design, Analysis, Modeling, and Testing XIX, 6941 1 69410C.
10. J.M Valeton, P.Bijl, E.Agterhuis and S. Kriekaard, "T-CAT, a new Thermal Camera Acuity Tester," Proc SPIE **4030**, 232 – 238 (2000).
11. W.A. Wagenaar, "Note on the construction of diagram-balanced Latin Squares, "Psychol. Bull. 72, 384–386 (1969).
12. P.Bijl and J.M. Valeton , "Guidelines for accurate TOD measurement. Proc SPIE **3701**, 14 - 25(1999).
13. K. Schutte , D.J. de Lange and S.P. van den Broek, "Signal conditioning algorithms for enhanced tactical sensor imagery," Proc SPIE **5076**, 92-100 (2003).
14. Vollmerhausen, R., & Driggers, R.G (1999). NVTherm: next generation night vision model. *Proc. IRIS Passive Sensors*, 1, 121-134.
15. Bijl, P. & Hogervorst, M.A. (2007). NVThermIP vs TOD: matching the Target Acquisition range criteria. *SPIE Proc. SPIE,* Vol. *6543*, pp. 65430C.
16. Driggers et al. (2006). Current infrared target acquisition approach for military sensor design and wargaming Infrared imaging systems. *Proc. SPIE,* Vol. 6207, pp. 620709.1-620709.17